1342

LBL-18552

NUMERICAL STUDIES OF FLUID AND HEAT FLOW NEAR HIGH-LEVEL NUCLEAR WASTE PACKAGES EMPLACED IN PARTIALLY SATURATED FRACTURED TUFF

by K. Pruess, Y. W. Tsang, and J. S. Y. Wang

Earth Sciences Division
Lawrence Berkeley Laboratory
University of California
Berkeley, California 94720

November 1984

ABSTRACT

We have performed modeling studies on the simultaneous transport of heat, liquid water, vapor, and air in partially saturated fractured porous rock. Formation parameters were chosen as representative of the potential repository horizon in the Topopah Spring Unit of the Yucca Mountain tuffs. The presence of fractures makes the transport problem very complex, both in terms of flow geometry and physics. The numerical simulator "TOUGH" used for our flow calculations takes into account most of the physical effects which are important in multi-phase fluid and heat flow. It has provisions for handling the extreme non-linearities which arise in phase transitions, component disappearances, and capillary discontinuities at fracture faces.

We model a region around an infinite linear string of nuclear waste canisters, taking into account both the discrete fractures and the porous matrix. From an analysis of the results obtained with explicit fractures, we develop "equivalent" continuum models which can reproduce the temperature, saturation, and pressure variation, and gas and liquid flow rates of the discrete fracture-porous matrix calculations. The "equivalent" continuum approach makes use of a generalized relative permeability concept to take into account the fracture effects. This results in a substantial simplification of the flow problem which makes larger scale modeling of complicated unsaturated fractured porous systems feasible. Potential applications for regional scale simulations and limitations of the continuum approach are discussed.

INTRODUCTION

Various rock types and geological settings are currently being studied in the U.S. to evaluate their suitability as a disposal medium for high-level nuclear wastes. The most likely mechanism by which radionuclides could reach the biosphere, should they ever escape from the engineered repository system, is through transport in groundwater after waste emplacement. Therefore, the hydrologic characteristics and mechanical stability of the host rock are of primary concern in the assessment of potential repository sites.

The tuff formations at the Nevada Test Site are unique among the candidate sites currently under investigation, in that the potential repository horizon is located above the water table in partially saturated rock. The very thick (up to 600 m) unsaturated zone offers a number of advantages for waste disposal in comparison to saturated rock of low permeability. The hydrogeologic and logistic factors favorable to the utilization of thick unsaturated zones for high-level waste disposal include (1) the probable absence of an effective mechanism to dissolve and transport the radionuclides to a deep water table or to the land surface under present arid climatic conditions, (2) probable protection from exhumation by erosion in a time frame of thousands of years, (3) availability of remote federally owned lands with suitable unsaturated zones, and (4) relative ease of placement and retrieval (Winograd, 1974).

The tuffs have both matrix and fracture porosity and permeability. At the potential repository horizon, 390 m below the ground surface, approximately 80% of the pore volume contains water, which is held in the porous matrix by capillary suction. The remaining voids contain air and a small amount of water vapor at ambient pressures and temperatures ($p \approx 1$ bar, $T \approx 26°C$).

To evaluate the suitability of the unsaturated zone as a disposal medium for high-level nuclear waste, one must consider the effects of a strong heat source upon liquid and gas movement in the unsaturated zone. We have applied a recently developed multi-phase multi-component code, TOUGH (Pruess, 1984), to model the effects of heat on the flow through discrete fractures and porous matrix around the waste. Based on understanding and insight gained from the discrete fracture-porous matrix simulations, we develop "equivalent" single continuum models to obtain a simplified description of the thermo-hydrologic response of a partially saturated fractured porous medium to nuclear waste emplacement.

NON-ISOTHERMAL UNSATURATED FLOW

The "conventional" description of unsaturated flow, as recently reviewed by Narasimhan (1982), was developed primarily by soil physicists. It assumes isothermal conditions and treats the gas phase as a passive spectator, which remains at constant pressure (1 bar) at all times. Liquid phase flows under gravity and capillary suction, as given by Richards' law (1931).

This approach has been extended to "weakly" non-isothermal systems (temperatures up to 50°C) by Philip and de Vries (1957), Sophocleous (1979), Milly (1982), and others. These authors consider moisture migration in the form of liquid or vapor. Vapor transport occurs only by molecular diffusion, and no overall movement of the gas phase is taken into account. The present status of "weakly" non-isothermal unsaturated flow has been reviewed by Walker, Sabey, and Hampton (1981), and Childs and Malstaff (1982).

Emplacement of high-level nuclear waste in partially saturated rock presents a "strongly" heat-driven problem, for which the approaches mentioned above are not applicable. Near the waste packages absolute temperatures may almost double (from ambient 300 K to near 600 K). From the ideal gas law $pV = nRT$ one then expects large increases in pressure and/or volume of the gas phase, which will give rise to strong forced convection of the gas phase from thermal expansion. Even stronger gas phase flow effects are expected from vaporization of liquid water, which will become vigorous when formation temperatures exceed 100°C.

To describe these phenomena it is necessary to employ a multi-phase approach to fluid and heat flow, which fully accounts for the movement of gaseous and liquid phases, their transport of latent and sensible heat, and

phase transitions between liquid and vapor. The gas phase will in general consist of a mixture of water vapor and air, and both these components must be kept track of separately.

We have developed a numerical simulator called "TOUGH" (transport of unsaturated groundwater and heat), which can represent most of the physical processes of significance in two-phase flow of water and air with simultaneous heat transport (Pruess, 1984). The formulation used in TOUGH is analogous to the multi-phase treatment customarily employed in geothermal reservoir simulators (Pruess, 1983; O'Sullivan et al., 1983). Similar numerical models have been recently developed, or are being developed by other authors (Travis, 1983; Eaton, 1983; Eaton et al., 1983; Hadley, private communication, 1984; Bixler, 1984). Table 1 summarizes the physical effects which impact on fluid and heat transport. Check marks indicate processes or effects which are presently accounted for in the governing equations solved by the TOUGH simulator. Processes which are checked off in parentheses are at present implemented in an approximate way. Other effects currently not accounted for in the computer model may be significant, and are being studied. The most important of these is probably Knudsen diffusion (in a different context known as "Klinkenberg effect"; Klinkenberg, 1941; Ertekin et al., 1983), which at low pressures is a more effective mechanism for gas transport in small pores than Darcy flow (Hadley, 1982; and personal communication). However, as most gas phase flow in the tuff takes place in fractures, the overall effects of Knudsen diffusion may well be minor.

The governing mass and heat balance equations solved in TOUGH are summarized in Appendix A. These equations are highly non-linear, because of order-of-magnitude changes in parameters during phase transitions, and because of

non-linear material properties (chiefly relative permeability for gas and liquid phases and capillary pressures). Furthermore, the mass- and energy-balance equations are strongly coupled. Because of these features of the equation system, TOUGH performs a completely simultaneous solution of the discretized mass- and energy-balance equations, taking all coupling terms into account. Space discretization is made with the integral finite difference method (IFD; Narasimhan and Witherspoon, 1976). Time is discretized fully implicitly as a first-order finite difference, to obtain the numerical stability needed for an efficient calculation of flow in fractures with extremely small volumes. Newton-Raphson iteration is performed to handle the non-linearities. The linear equations arising at each iteration step are solved directly, using Gaussian elimination and sparse storage techniques (Duff, 1977). The numerical performance of TOUGH was verified by comparison with a number of geothermal reservoir and unsaturated flow problems for which analytical or numerical solutions are available (Pruess and Wang, 1984).

DESCRIPTION OF FLOW IN FRACTURED ROCKS

A substantial complication of the flow problem considered here arises from the complex geometric characteristics of fractured rock with significant matrix porosity and permeability. Numerical modeling of fluid and heat flow in fractured media can be approached in several different ways. Conceptually it is most straightforward to model the discrete fractures explicitly, using small volume elements together with porous matrix blocks. Flow through a fracture with effective aperture δ can be approximated by Darcy's law with permeability $k_f = \delta^2/12$ (Witherspoon et al., 1980). The explicit discretization approach to modeling flow in fractured media is suitable for fundamental studies of idealized systems, but it is not practical for most "real" problems, where the amount of geometric detail and complexity is far beyond the capacity of digital computers. Even if computationally feasible, a detailed explicit treatment of all fractures would hardly seem desirable in practice. Available field data on fracture distributions are typically rather incomplete. Moreover, in modeling thermohydrological conditions one is usually interested in predicting averages over some macroscopic scale, and too much detail on the level of individual fractures would be useless.

A powerful approach to modeling of flow in fractured media is the double-porosity method, originally developed by Russian hydrologists (Barenblatt et al., 1960), and introduced into the petroleum literature by Warren and Root (1963). In this method, a fractured porous medium is partitioned into (1) a primary porosity, which consists of small pores in the rock matrix, e.g. intergranular vugs or vesicles, and (2) a secondary porosity, consisting of fractures and joints. Each of the two porosities is treated as a continuum,

whose properties can be characterized by means of the customary porous medium properties, i.e., permeability, porosity, and compressibility. Flow within each continuum is assumed to be porous flow, governed by Darcy's law. The global flow in the medium occurs only through the fracture continuum, while fractures and rock matrix may interact locally by means of "interporosity" flow. In the classical double-porosity work, a quasi-steady approximation was made for interporosity flow, which is usually satisfactory for problems involving isothermal single-phase flow (Moench, 1983). However, in problems involving multi-phase fluids with large and varying compressibility, and coupled fluid and heat flow, the period of transient flow between matrix and fractures can be very long. For this type of problem, the double-porosity method was extended to a method of multiple interacting continua (MINC) by Pruess and Narasimhan (1982a, b). The MINC-method treats interporosity flow in a fully transient way, using numerical methods.

While yielding a substantial simplification for modeling, the double-and multiple-porosity methods when applied to simulating thermohydrological conditions near high-level waste packages still require a very large amount of computational work. The explicit representation of interporosity flow adds an extra dimension to the flow problem; furthermore, the extremely small average porosity of the fracture network slows computations down drastically, due to throughput limitations in grid blocks of very small volume.

It would be desirable to go one step further and attempt to approximate the fluid and heat flow in a fractured medium by means of a single effective or "equivalent" continuum. Possibilities and limitations for representing the permeability of a fracture system by means of an equivalent porous medium

have been studied by Long et al. (1982). These authors have considered steady isothermal single-phase flow in fracture networks, with completely impermeable matrix. In our case, extensive boiling of formation water occurs in the matrix, so that matrix permeability and porosity cannot be ignored. The problem of developing an "equivalent" continuum description for multi-phase flow in a fractured porous medium is considerably more difficult than the problem of single-phase, fracture-only flow. In this study, we attempt to develop single "equivalent" continuum models by suitable choice of permeabilities for gas and liquid flows. An "equivalent" continuum may be defined as one that will yield the same mass fluxes, and temperature, pressure, and saturation distributions as an explicit discrete fracture-porous matrix model, given the same initial and boundary conditions.

However, two problems associated with the equivalent continuum concept arise immediately. The first relates to porosity. Typically, matrix porosity may be 1-2 orders of magnitude larger than fracture porosity. If continuum porosity is chosen as the sum of matrix and (average) fracture porosity, then fracture flow velocities would be underpredicted by similar factors. If alternatively continuum porosity were chosen equal to the average porosity of the fracture system, then the relationship between mass fluxes and flow velocities in the fractures would be preserved, but formation water content would be underpredicted by 1-2 orders of magnitude. This is clearly unacceptable when considering processes which involve extensive boiling of formation water. The second problem of defining an "equivalent" continuum is associated with the driving forces of two-phase flow. Ignoring diffusive transport for the moment, gas flow occurs in response to pressure and gravity forces, whereas

liquid phase flow is in addition affected by capillary forces. In a fractured porous medium, there is a continuous variation of pressures between fractures and matrix, whereas in a single continuum model only one pressure is defined for each phase at each point (i.e. in a suitably chosen region around each point). Therefore, if the equivalent continuum description is chosen such as to preserve the gas fluxes in the fractures for the fractured porous system, then the driving forces for liquid flow in the matrix will be altered.

From the above considerations it is clear that in the case of multi-phase flow in a fractured porous medium, an "equivalent" continuum description with a single porosity may be of limited utility in modeling flow velocities and driving forces. It appears that, to avoid basic inconsistencies, at least two continua are required for an acceptable representation of flow. However, because of the computational complexities of even the simplest two-continua model, we believe it worthwhile nonetheless to attempt to develop single continuum models which can adequately predict certain aspects of the thermo-hydrological response to waste emplacement.

MODELING APPROACH

The general approach followed in the present work is as follows. As a first step, we perform detailed modeling studies of fluid and heat flow near waste packages emplaced in fractured porous tuff, using an explicit representation of fractures. To accomplish such modeling it is necessary to idealize fracture and waste emplacement geometry to a considerable degree. Specifically, we consider only one set of plane, parallel, infinite fractures, which intersect an infinite linear string of waste packages at a right angle (Figure 1). Apart from this idealization we do employ geometric and matrix hydrologic parameters which, although preliminary, have been suggested as representative of actual values for the system under study (Keith Johnstone, private communication, 1983). However, hydrologic properties of the fractures are rather poorly known at present. Therefore, two hypothetical cases are studied to explore possible system behavior.

These explicit fracture studies provide a detailed "microscopic" look at system evolution after waste emplacement. The results obtained, while of interest in their own right, then serve as "benchmarks" in a second step, where we generate fluid and heat flow predictions for various single-continuum models in search for an "equivalent" continuum. Specifically, based on the process characteristics observed in the explicit fracture models, we propose single-continuum parameters which might be expected to yield a behavior similar to the explicit fracture model. The continuum models are tested by comparing predictions for temperatures, pressures, saturation profiles, mass and heat flow rates etc. with those obtained in the explicit fracture models. In this way it is possible to evaluate utility and validity of the continuum models.

SPECIFICATION OF THE EXPLICIT DISCRETE FRACTURE-POROUS MATRIX STUDIES

In the calculations reported here we neglect gravity and infiltration effects. For the idealized geometry shown in Figure 1, it is then only necessary to model a symmetry element, as indicated by dashed lines. However, for convenience we will quote results for extensive quantities such as fluid and heat flow rates on a "per waste package" basis. Most of the formation parameters used in the calculations are summarized in Table 2 (Keith Johnstone, private communication, 1983). These parameters represent preliminary data for the densely welded, devitrified, non-lithophysal zone of the Topopah Spring Unit of the Yucca Mountain tuffs. Characteristic curves (relative permeability and suction pressure) are only given for the rock matrix. No data are available for the characteristic curves in the fractures. To arrive at the characteristic curves for the fractures in our calculations, we proceed as follows.

Upon close examination of the measured suction curve for the tuff matrix as shown in Figure 2, we note that the very strong suction pressures such as -2000 bars at low liquid saturation in the matrix ($S_{\ell,m}$ = 2%) cannot represent effects of capillary pressure related to the curvature of the matrix pores. (Indeed, the capillary radius corresponding to P_{suc} = -2000 bars is 7.3×10^{-8} cm, or approximately twice the diameter of a water molecule!). In this range of low liquid saturation the suction curve in fact represents the effects of liquid phase adsorption on the solid surface of the rock. The transition from capillary mechanism to adsorption mechanism has been studied in concrete slabs (Huang et al. 1979). Since the adsorption mechanism depends only on the physical-chemical properties of the rock-liquid interaction, but

not on the curvature of the pore surfaces, we expect that the same effects are present on the fracture surfaces as on the matrix pore surfaces at low liquid saturations. At the ambient suction P_{suc} = -10.93 bar for the matrix at initial liquid saturation $S_{\ell,m}$ = 80%, the liquid cannot be held by capillary force in the fractures. If we apply the expression, $P_{cf} = -2\sigma/\delta$, to the fracture, where σ is the surface tension and δ is the fracture aperture, we obtain at ambient temperature P_{cf} = -.00073 bar, which is much smaller than the ambient suction P_{suc} = -10.93 bar. Therefore, liquid can be present on the fracture surfaces only as a thin film of a few molecular layers. We propose that the very strong suction pressures at low liquid saturation for the matrix shown in Figure 2 are also encountered when the fractures are desaturated, except that most of this pressure range corresponds to a small interval of low liquid saturations in the fractures.

The thin film of liquid on the fracture walls presumably has extremely low mobility. Specifically, we assume an immobile saturation $S_{\ell r}$ such that liquid relative permeability in the fracture $k_{r\ell}$ (S_ℓ) = 0 for $S_\ell < S_{\ell r}$. For $S_\ell > S_{\ell r}$, the liquid and gas fracture relative permeabilities are assumed to be linear functions of saturations and to obey the relationship $k_{r\ell} + k_{rg} = 1$ as suggested in the geothermal literature (Pruess et al., 1983). For definiteness and convenience we assume an immobile $S_{\ell r}$ = 1%; however, neither this particular value nor the assumption of a vanishing relative permeability for $S_\ell < S_{\ell r}$ are essential for our numerical experiments.

As quantitative information on the suction pressures for fractures at low saturations is not presently available, we consider two cases which are intended to illustrate alternative possible system behavior. These cases

differ in respect to mobility of liquid in the fractures at the initial (pre-emplacement) liquid saturation. In the first case we assume for simplicity that $P_{suc,f}$ varies linearly between 0 and the limiting value of -5000 bars used in the matrix for the saturation interval $0.01 > S_\ell > 0$. Before canister emplacement, matrix and fractures will be in capillary equilibrium. At the assumed initial matrix saturation of $S_{\ell,m} = 80\%$ we have $P_{suc} = -10.93$ bars. This value is attained in the fractures at a liquid saturation of $S_{\ell,f} = .9878\%$, which we use as initial condition in our problem. Note that this saturation is just barely below the assumed irreducible liquid saturation in the fractures of $S_{\ell r} = 1.0\%$, so that initially liquid is immobile in the fractures (see Figure 3).

In the second case we assume that the linear variation of P_{suc} with S_ℓ occurs over a larger range, namely, $0 < S_\ell < 0.05$, so that capillary equilibrium between matrix and fractures is attained at a saturation $S_\ell > S_{\ell r}$, and liquid is (slightly) mobile in the fracture at initial conditions. One of the most numerically difficult aspects of the first case, where P_{suc} varied from 0 to -5000 bars in the range of $0.01 > S_\ell > 0$, is the extremely large slope $dP_{suc}/dS_\ell = 5 \times 10^5$ bars. To facilitate calculations in the second case we arbitraily diminish maximum strength of suction pressure to -50 bars, giving a more modest slope of $dP_{suc}/dS_\ell = 50/.05 = 10^3$ bars. As it turns out in the simulation, liquid saturation in the fracture never changes by more than 1.2×10^{-3} %, so that only the slope dP_{suc}/dS_ℓ is of significance here, whereas maximum absolute strength of P_{suc} is irrelevant. Initial capillary equilibrium in Case 2 is attained at $S_{\ell,f} = 3.928\%$, at which saturation liquid relative permeability is $k_{\ell,f} = 2.96 \times 10^{-2}$.

The calculations were carried out using a two-dimensional r - z grid, with parameters as given in Table 3.

RESULTS OF DISCRETE FRACTURE-POROUS MATRIX STUDIES

We shall first describe the simulated response of the porous fractured system to waste package emplacement in a general way as shown schematically in Figure 4. Detailed discussion of the computed results will be given in conjunction with introduction of equivalent continuum concepts and parameters below.

Emplacement of waste packages causes temperatures to rise in both rock matrix and fractures. Initially this causes evaporation of a modest amount of liquid water, as partial pressure of vapor increases according to the saturation curve $P_v \simeq P_{sat}(T)$. Boiling becomes vigorous as the temperature reaches 100°C. Most of the vapor generated in the rock matrix flows towards the fractures, and then flows radially outward in the fractures, where it soon condenses on the cooler walls of the rock. In Case 1, where liquid is initially immobile in the fractures, the condensed liquid re-enters the matrix under capillary suction, and then migrates down the saturation profile towards the boiling region near the waste package. However, because of low matrix permeability, radial outflow of vapor in the fractures exceeds radial inflow of liquid in the matrix, so that the rock near the waste package becomes desaturated (dries up). As time progresses the entire spatial pattern of vaporization in the matrix, vapor discharge into the fractures, condensation at fracture walls and liquid backflow in the matrix towards the heat source slowly migrates radially outward, away from the canister. Even though liquid is only barely immobile in the fractures initially, it remains immobile at all times. The very slight saturation buildup of $\Delta S_{\ell,f} > 0.0122\%$ required to achieve liquid mobility in the fractures is never accomplished, because capillary suction in

the matrix is sufficiently strong to draw liquid out of the fractures at the same rate as it condenses.

The behavior of the condensed liquid is entirely different in the second case, where liquid has a finite mobility in the fractures. The slight saturation increase in the fractures as a consequence of condensation induces a suction gradient and associated liquid flux in the fracture. The extremely large fracture permeability gives rise to rapid movement of water away from the condensation front, both radially inward and outward. In this way the condensed water is rapidly distributed over the fracture faces, with little water entering the matrix near the condensation front. Backflow of liquid towards the boiling region near the canister is facilitated by the high-permeability pathway in the fractures. With time a balanced vapor-liquid counterflow is established, which stabilizes the saturation profile near the canister, and prevents the drying process from going very far. This suction-driven two-phase counterflow represents an extremely efficient heat transfer mechanism known as "heat pipe" (Eastman, 1968). In the present case, the "overpressure" needed to drive the heat pipe is small because of the large fracture permeability. Gas phase pressures always remain close to 1 bar, so that temperatures in the fractures remain near or below 100°C. Because of the small fracture spacing the pathways for vapor flow and heat conduction from the rock matrix to the fractures are short (< 11cm) and temperature and pressure conditions remain close to (T, P) = (100°C, 1 bar) even in the rock matrix. This is in contrast to Case 1 where the temperature rises to much higher values.

EQUIVALENT CONTINUUM MODELS

We shall now examine in detail the simulated fluid and heat flow processes in a fractured porous medium in an attempt to identify the specific effects of fractures, and to approximate these effects by means of a single continuum with suitably chosen "effective" hydrologic parameters.

Calculated results for Case 1 are given in Figures 5 through 9, and for Case 2 in Figures 10 through 14. For comparison we have also included results for porous medium models with no allowance for fractures, as well as for "equivalent" continuum models, to be described below.

For Case 1 with liquid immobile in the fractures at all times, it appears that the role of the fractures is solely to provide a high-permeability pathway for gas phase flow, while having no effects on liquid flow. This suggests a very simple prescription for effective continuum parameters which should be able to represent these effects. Namely, we prescribe a very large relative permeability $k_{rg} = 3067$ for the gas phase, so that effective gas permeability $k_{rg} \cdot k_m = 10^{-13}\ m^2$ is equal to the average continuum permeability $\overline{k_f}$ of the fractures, independent of saturation. We make no changes whatsoever in the other rock matrix parameters. Calculated results from this model are labeled "porous matrix with large effective gas permeability" in Figures 5 through 9. Comparison with the detailed fracture calculation, and with porous medium calculations without fractures, reveals the following trends.

There is excellent agreement between the calculation using explicit fractures and the "equivalent" continuum with large gas permeability in all important parameters, i.e., temperatures, pressures, liquid saturation, and gas and liquid flow rates. In each figure, the intensive quantities, tempera-

ture, pressure and saturation, from the explicit discrete fracture-porous matrix calculations are averaged over the grid layers at each radius and the extensive flow rates are summed over the grid layers for meaningful comparison with continuum models. The results obtained from the "no fractures" calculation (unmodified rock matrix parameters) are generally rather different. Saturation and pressure profiles, as well as flow rates of gas and liquid, show rather dramatic fracture effects which are very well reproduced by the "equivalent" continuum model with large gas permeability. Temperatures are not very strongly affected by the presence of fractures in this case with immobile water in the fractures, because of absence of sufficient permeability for water flow.

For Case 2 with liquid mobile in the fractures, the role of the fractures is to provide high-permeability pathways for both the liquid flow and the gas flow while the matrix acts as the fluid source. To approximate the fracture effects by means of an equivalent continuum, we modify two rock matrix parameters: the relative permeability for liquid flow and the relative permeability for gas flow. We assign for the liquid flow the relative permeability $k_{r\ell} = 90.65$, so that the effective liquid permeability $k_{r\ell} \cdot k_m = (k_{r\ell,f}) \cdot \overline{k}_f = 2.96 \times 10^{-15}$ m^2, where $k_{r\ell,f} = 2.96 \times 10^{-2}$ is the relative permeability for liquid flow along discrete fractures at initial saturation, and $\overline{k}_f$ is the average continuum permeability of the fractures. We also assign for the gas flow a large relative permeability $k_{rg} = 2976.35$ so that $k_{rg} \cdot k_m = (k_{rg,f}) \cdot \overline{k}_f$. As in Case 1, all other formation parameters are the same as for the porous medium model without fractures. Calculated results from the mobile liquid "equivalent" continuum model are labeled "porous continuum with large effective liquid and gas permeabilities" in Figures 10 through 14.

There is again excellent agreement between the calculation using explicit fractures and the "equivalent" continuum with large liquid and gas permeabilities in temperatures, liquid saturation in the matrix, gas and liquid flow rates, and pressures in the fractures. The discrete fracture calculations show that vapor condensation on the fracture walls never changes liquid saturation in the fracture by more than 1.2×10^{-3} %, indicating that the suction pressure gradient is sufficiently strong to rapidly distribute the liquid over the fracture surfaces. The nearly constant saturation makes it possible to use the initial effective liquid permeability $(k_{r\ell,f})\cdot\overline{k}_f$ to determine the constant relative permeability for the "equivalent" continuum model. Near the canister with intensive boiling in the matrix, the pressure in the matrix is slightly higher than in the fractures, which is the driving mechanism for the gas flow from the matrix to the fractures (see Figure 12). This interporosity flow normal to the matrix-fracture interfaces is not accounted for in the "equivalent" continuum model. Away from the immediate vicinity of the waste canisters, the "equivalent" continuum model with large liquid and gas permeabilities faithfully reproduces the movements of gas and liquid. Figures 10 through 14 show that the results from the "no fractures" calculation are quite different from the models taking fractures into account. With liquid mobile in the fractures, the temperature near the waste canister will remain close to 100°C, and the thermally induced liquid flow can easily move away from the condensation front into the formation.

CODE PERFORMANCE

Fluid and heat flow calculations with explicit representation of fractures require a large amount of numerical work, because the interporosity flow

between rock matrix and fractures adds an extra dimension to the flow problem, and because attainable time step sizes are restricted by the small volume elements representing fractures. The whole point of introducing an equivalent continuum description is to obtain an approximation to the fractured porous flow problem which provides acceptable accuracy, while at the same time reducing the numerical work, so that calculations for realistic emplacement geometries and for time spans of thousands of years become feasible.

In Table 4 we compare computing times for the various runs. It is seen that the equivalent continuum calculations in both cases are faster than the explicit fracture calculations by a factor of approximately 20. For the equivalent continuum, numerical work per time step is reduced by a factor of approximately 4.5 (which is close to the ratio of the number of grid blocks), while average time step size is increased by a similar factor. In Case 1 the equivalent continuum calculation is a factor 2.5 slower than the porous medium calculation, while in Case 2 it is slightly faster. These differences arise from different time step sizes; the CPU-times per time step are rather similar in all one-dimensional calculations. The large gas relative permeability used in the equivalent continuum in Case 1 limits time steps in comparison to the porous medium model. In Case 2 with constant relative permeability for gas and liquid somewhat larger time steps are possible than for the porous medium with highly non-linear (although smaller) relative permeabilities.

DISCUSSION

Our calculations show that in the presence of a strong heat source in a partially saturated fractured porous formation, the flow of gas (vapor/air) is dominated by fracture effects. Liquid flow is significantly affected by the

fractures only if liquid is mobile in the fractures. Our modeling studies indicate that the fracture effects can be represented in a single effective continuum by choosing appropriate gas and liquid relative permeabilities.

In modeling two alternative system behaviors (one with liquid immobile and the other with liquid mobile in the fractures), we show that if the liquid is initially mobile in the fractures the rock temperature will remain close to 100°C; while temperatures rise to much higher values when there is no liquid mobility in the fracture initially. This result suggests that stabilization of rock temperatures near 100°C is a characteristic signature of conditions where liquid is initially mobile in the fractures. With liquid mobile in the fractures, the thermally induced liquid movement occurs over a much larger region than in the case with no liquid mobility in the fractures.

In focusing on the interplay of pressure driving force and suction driving force in this study, we have neglected gravity effects. We are currently extending the equivalent continuum modeling studies, with inclusion of gravity, to examine the thermohydrological response to nuclear waste emplacement on a regional scale. For large scale modeling, it is necessary to use "equivalent" continuum models as it is impractical to model all the discrete fractures together with the porous matrix. The results presented in this report suggest that fracture effects on a regional scale can be adequately handled by means of equivalent continuum models, resulting in order-of-magnitude savings in computing work.

The effective hydrologic parameters for an "equivalent" continuum depend not only on formation parameters, but also upon initial thermodynamic conditions, such as initial moisture content. Moreover, the effective continuum

parameters will also depend upon the particular flow process considered, and upon the nature of the perturbation to which the fractured porous medium is subjected. The processes considered in this report have the simple characteristic that liquid saturations in the fractures never change by more than a minute amount. It is this feature which makes possible a simple effective continuum representation in terms of (large) effective relative permeabilities. For other types of processes, such as major flood events with large saturation transients in the fractures, such simplification may not be applicable. In that case it may in fact not be possible to obtain an equivalent continuum description.

In conclusion, it should be emphasized that single continuum models can predict only certain aspects of the thermohydrologic response. We have demonstrated that "equivalent" continuum models can reproduce the temperature, pressure, saturation, and fluid flow fields generated from waste emplacement. However a single continuum gives only a single velocity field, which will either underestimate flow velocities in the fractures or overestimate flow velocities in the matrix. Furthermore, no description of interflow between fractures and matrix is made in the single continuum model. These deficiencies of the "equivalent" continuum approach may have a strong impact on predictions for transport of chemical species. Therefore, the utility of continuum models for predicting contaminant transport is uncertain at the present time.

ACKNOWLEDGEMENT

This work was supported, in part, by the NNWSI Performance Assessment Division, Sandia National Laboratories, and by the Director, Office of Energy Research, Office of Basic Energy Sciences, of the U. S. Department of Energy under Contract No. DE-AC03-76SF00098.

Table 1: Physical Processes in Strongly Heat-Driven Flow in Partially Saturated Rocks

1. Fluid Flow
   - ✓ pressure forces
   - ✓ viscous forces
   - inertial forces
   - ✓ gravity
   - ✓ interference between liquid and gas
   - ✓ dissolution of air in liquid
   - ✓ capillarity and adsorption
   - differential heat of wetting } liquid
   - chemical potential gradients
   - ✓ mixing of vapor and air
   - ✓ vapor pressure lowering
   - ✓ binary diffusion } gas
   - Knudsen diffusion
   - thermodiffusion

2. Heat Flow
   - ✓ conduction
   - ✓ flow of latent and sensible heat
   - radiation

3. Vaporization and Condensation
   - ✓ temperature and pressure effects
   - ✓ capillarity and adsorption

4. Changes in Rock Mass
   - (✓) thermal expansion
   - (✓) compression under stress
     thermal stress cracking
   - (✓) change in porosity and
     permeability

Table 2: Formation Parameters

Matrix	
rock grain density	$\rho_R = 2550$ kg/m^3
rock specific heat	$C_R = 768.8$ J/kg°C
rock heat conductivity (dry)	$K = 1.6$ W/m°C
porosity	$\phi_m = 10.3$ %
permeability	$k_m = 32.6 \times 10^{-18}$ m^2
suction pressure	$P_{suc}(S_\ell) = -1.393\ (S_{EF}^{-1/\lambda}-1)^{1-\lambda}$ MPa
relative permeability to liquid (van Genuchten, 1980)	$k_{r\ell}(S_\ell) = \sqrt{S_{EF}}\ [1-(1-S_{EF}^{1/\lambda})^{\lambda}]^2$
relative permeability to gas	$k_{rg}(S_\ell) = 1 - k_{r\ell}$
	where $S_{EF} = (S_\ell - S_{\ell r})/(1 - S_{\ell r})$, $S_{\ell r} = 9.6 \times 10^{-4}$, $\lambda = 0.45$
Fractures (one vertical set)	
aperture	$\delta = 2$ mm
porosity	$\phi_f = 20$ %
spacing	$D = .22$ m
average continuum permeability	$\bar{k}_f = 10^{-13}$ m^2
permeability per fracture*	$k_f = \bar{k}_f \cdot D/\delta = 11 \times 10^{-12}$ m^2
equivalent continuum porosity	$\bar{\phi}_f = \phi_f \delta/D = 0.182$ %
Initial Conditions	
temperature	$T = 26$ °C
pressure	$p = 10^5$ Pa (≡ 1 bar)
liquid saturation in matrix	$S_{\ell,m} = 80$ %

*Note that we do not imply a parallel-plate model for the fractures; k_f is less than the parallel plate permeability $(\phi_f \delta)^2/12 = 1.33 \times 10^{-8}$ m^2.

Table 3: Computational Grid for Explicit Fracture Calculations.

The grid has a height of h = 0.11 m, corresponding to half the fracture spacing. It extends from the wall of the canister (r = 0.25 m) out to r = 300 m, at which distance boundary conditions of T = 26°C, p = 1 bar, S_ℓ = 0.80 are maintained. Discretization in r - direction is made with a series of concentric cylinders with the following radii.

grid element	radius (m)	grid element	radius (m)	grid element	radius (m)
1	.2700	17	3.096	31	38.49
2	.3050	18	3.563	32	45.24
3	.3660	19	4.465	33	53.12
4	.4359	20	5.517	34	62.33
5	.5159	21	6.747	35	73.07
6	.6075	22	8.182	36	85.62
7	.7124	23	9.857	37	100.3
8	.8326	24	11.81	38	117.4
9	.9702	25	14.10	39	137.3
10	1.128	26	16.76	40	160.6
11	1.308	27	19.88	41	187.8
12	1.515	28	23.51	42	219.6
13	1.751	29	27.75	43	256.7
14	2.023	30	32.71	44	300.0
15	2.334				
16	2.689				

In z-direction we discretize into four layers, the first of which represents (half of) the fracture:

layer	thickness (m)
A	1×10^{-3}
B	4×10^{-3}
C	1.5×10^{-2}
D	9.0×10^{-2}

Table 4: TOUGH Performance Measures

	Explicit fractures	Equivalent continuum	Porous medium
Problem dimensionality	2-D	1-D	1-D
Number of grid blocks	173	44	44
Case 1 - immobile liquid in fractures			
physical time	160.37 D	153.70 D	153.70 D
CPU - time*	1897.20 s	106.09 s	41.45 s
time-steps	170	40	17
average time-step size	0.9434 D	3.843 D	9.041 D
CPU - time per time-step	11.16 s	2.652 s	2.438 s
Case 2 - mobile liquid in fractures			
physical time	365.25 D	365.25 D	365.25 D
CPU -time*	1144.95 s	51.80 s	61.51 s
time-steps	97	21	28
average time step-size	3.765 D	17.39 D	13.04 D
CPU-time per time-step	11.80 s	2.467 s	2.197 s

*On Lawrence Berkeley Laboratory's CDC-7600 machine

REFERENCES

Barenblatt, G. E., Zheltov, I. P., and Kochina, I. N., 1960, Basic Concepts in the Theory of Seepage of Homogeneous Liquids in Fissured Rocks, J. Appl. Math. (USSR), Vol. 24, No. 5, pp. 1286-1303.

Bixler, N. E., 1984, NORIA - A Finite Element Computer Program for Analyzing Water/ Vapor/Air/Energy Transport in Porous Media, Sandia National Laboratories, SAND report in preparation, Albuquerque, NM.

Childs, S. W., and Malstaff, G., 1982, Final Report: Heat and Mass Transfer in Unsaturated Porous Media, Pacific Northwest Laboratory, Report PNL-4036, Richland, WA, February.

Duff, I. S., 1977, MA28 - A Set of FORTRAN Subroutines for Sparse Unsymmetric Linear Equations, AERE Harwell Report R 8730, July.

Eastman, G. Y., 1968, The Heat Pipe, Scientific American, Vol. 218, pp. 38-46.

Eaton, R. R., 1983, A Numerical Method for Computing Flow through Partially Saturated Porous Media, paper presented at International Conference on Numerical Methods in Thermal Problems, Seattle, WA, August.

Eaton, R. R., Gartling, D. K., and Larson, D. E., 1983, SAGUARO - A Finite Element Computer Program for Partially Saturated Porous Flow Problems, Sandia National Laboratories, Report SAND82-2772, Albuquerque, NM, June.

Edlefsen, N. E., and Anderson, A.B.C., 1943, Thermodynamics of Soil Moisture, Hilgardia, Vol. 15, No. 2, pp. 31-298.

Ertekin, T., King, G. R., and Schwerer, F. C., 1983, Dynamic Gas Slippage: A Unique Dual-Mechanism Approach to the Flow of Gas in Tight Formations, paper SPE-12045, presented at the Society of Petroleum Engineers 58th Annual Technical Conference and Exhibition, San Francisco, CA.

Hadley, R. G., 1982, Theoretical Treatment of Evaporation Front Drying, Int. J. Heat Mass Transfer, Vol. 25, No. 10, pp. 1511-1522.

Hirschfelder, J. O., Curtiss, C. F., and Bird, R. B., 1954, Molecular Theory of Gases and Liquids, John Wiley and Sons, New York.

Huang, C. L. D., Siang, H. H., and Best, C. H., 1979, Heat and Moisture Transfer in Concrete Slabs, Int. J. Heat Mass Transfer, Vol. 22, pp. 257-266.

International Formulation Committee, 1967, A Formulation of the Thermodynamic Properties of Ordinary Water Substance, IFC Secretariat, Düsseldorf, Germany.

Klinkenberg, L. J., 1941, The Permeability of Porous Media to Liquids and Gases, in: API Drilling and Production Practice, pp. 200-213.

Long, J. C. S., Remer, J. S., Wilson, C. R., and Witherspoon, P. A., 1982, Porous Media Equivalents for Networks of Discontinuous Fractures, Water Resources Research, Vol. 18, No. 3, pp. 645-658.

Milly, P. C. D., 1982, Moisture and Heat Transport in Hysteretic, Inhomogeneous Porous Media: A Matric-Head Based Formulation and a Numerical Model, Water Resources Research, Vol. 18, No. 3, pp. 489-498.

Moench, A. F., 1983, Well Test Analysis in Naturally Fissured, Geothermal Reservoirs with Fracture Skin, in: Proceedings, Ninth Workshop on Geothermal Reservoir Engineering, Stanford University, Stanford, CA.

Narasimhan, T. N., and Witherspoon, P. A., 1976, An Integrated Finite Difference Method for Analyzing Fluid Flow in Porous Media, Water Resources Research, Vol. 12, No. 1, pp. 57-66.

Narasimhan, T. N., 1982, Physics of Saturated-Unsaturated Subsurface Flow, in: T. N. Narasimhan (ed.), Recent Trends in Hydrogeology, The Geological Society of America, Special Paper 189.

O'Sullivan, M. J., Bodvarsson, G. S., Pruess, K., and Blakeley, M. R., 1983, Fluid and Heat Flow in Gas-Rich Geothermal Reservoirs, paper SPE-12102, presented at the Society of Petroleum Engineers 58th Annual Technical Conference and Exhibition, San Francisco, CA., October (to appear in Soc. Pet. Eng. J.).

Philip, J. R., and de Vries, D. A., 1957, Moisture Movement in Porous Materials under Temperature Gradients, EOS Trans. AGU, Vol. 38, No. 2, pp. 222-232.

Pruess, K., 1983, Heat Transfer in Fractured Geothermal Reservoirs with Boiling, Water Resources Research, Vol. 19, No. 1, pp. 201-208, February.

Pruess, K., 1984, TOUGH - A Numerical Model for Strongly Heat Driven Flow in Partially Saturated Media, LBL Earth Sciences Division Annual Report, pp. 39-41, also paper in preparation.

Pruess, K., Bodvarsson, G. S., and Stefansson, V., 1983, Analysis of Production Data From the Krafla Geothermal Field, Iceland, in: Proceedings, Ninth Workshop on Geothermal Reservoir Engineering, Stanford University, Stanford, CA.

Pruess, K., and Narasimhan, T. N., 1982a, On Fluid Reserves and the Production of Superheated Steam from Fractured, Vapor-Dominated Geothermal Reservoirs, Journal of Geophysical Research, Vol. 87, No. B11, pp. 9329-9339.

Pruess, K., and Narasimhan, T. N., 1982b, A Practical Method for Modeling Fluid and Heat Flow in Fractured Porous Media, Proceedings Sixth SPE-Symposium on Reservoir Simulation, paper SPE-10509, New Orleans, LA., February (to appear in Soc. Pet. Eng. J.).

Pruess, K., and Wang, J. S. Y., 1984, TOUGH - A Numerical Model for Nonisothermal Unsaturated Flow to Study Waste Canister Heating Effects, in: G.L. McVay (ed.), Mat. Res. Soc. Symp. Proc., Vol. 26, Scientific Basis for Nuclear Waste Management, p. 1031-1038, North Holland, New York.

Richards, L. A., 1931, Capillary Conduction of Liquids through Porous Mediums, Physics, Vol. 1, pp. 318-333.

Sophocleous, M., 1979, Analysis of Water and Heat Flow in Unsaturated-Saturated Porous Media, Water Resources Research, Vol. 15, No. 5, pp. 1195-1206.

Travis, B. J., 1983, WAFE: A Model for Two-Phase Multi-Component Mass and Heat Transport in Porous Media, draft report, Los Alamos National Laboratory.

van Genuchten, M. Th., 1980, A Closed-Form Equation for Predicting the Hydraulic Conductivity of the Unsaturated Soils, Soil Sci. Soc. Am. J., Vol. 44, pp. 892-898.

Walker, W. R., Sabey, J. D., and Hampton, D. R., 1981, Studies of Heat Transfer and Water Migration in Soils, Final Report, Department of Agricultural and Chemical Engineering, Colorado State University, Fort Collins, CO., 80523, April.

Warren, J. E., and Root, P. J., 1963, The Behavior of Naturally Fractured Reservoirs, Soc. of Pet. Eng. J., pp. 245-255, September.

Winograd, I. J., 1974, Radioactive Waste Storage in the Arid Zone, EOS, Transactions of the American Geophysical Union, Vol. 55, No. 10, pp. 884-894, October.

Witherspoon, P. A., Wang, J. S. Y., Iwai, K., and Gale, J. E., 1980, Validity of Cubic Law for Fluid Flow in a Deformable Rock Fracture, Water Resources Research, Vol. 16, No. 6, pp. 1016-1024.

APPENDIX A: Mass and Energy Balances

TOUGH solves discretized versions of the following mass- and energy-balance equations

$$\frac{d}{dt}\int_{V_n} M^{(\kappa)}dv = \int_{\Gamma_n} \underset{\sim}{F}^{(\kappa)} \cdot \underset{\sim}{n}\, d\Gamma + \int_{V_n} q^{(\kappa)}\, dv \qquad (1)$$

(κ=1: water; κ=2: air; κ=3: heat)

The mass accumulation terms (κ=1,2) are

$$M^{(\kappa)} = \phi \sum_{\beta=\ell,g} S_\beta \rho_\beta X_\beta^{(\kappa)} \qquad (2)$$

where ϕ is porosity, S_β is saturation of phase β (= liquid, gas), ρ_β is density of phase β, and $X_\beta^{(\kappa)}$ is the mass fraction of component κ present in phase β. The heat accumulation term contains rock and fluid contributions

$$M^{(3)} = (1-\phi)\rho_R C_R T + \phi \sum_{\beta=\ell,g} S_\beta \rho_\beta u_\beta \qquad (3)$$

where ρ_R is rock grain density, C_R is rock specific heat, T is temperature, and u_β is specific internal energy of phase β.

The mass flux terms contain a sum over phases

$$\underset{\sim}{F}^{(\kappa)} = \sum_{\beta=\ell,g} \underset{\sim}{F}_\beta^{(\kappa)} \qquad (4)$$

where the flux in each phase is

$$\underset{\sim}{F}_\beta^{(\kappa)} = -k \frac{k_{r\beta}}{\mu_\beta} \rho_\beta X_\beta^{(\kappa)} (\nabla P_\beta - \rho_\beta \underset{\sim}{g}) - \phi_{\beta g} D_{va} \nabla \left(X_\beta^{(\kappa)} \rho_\beta \right) \qquad (5)$$

Here k is absolute permeability, $k_{r\beta}$ is relative permeability of phase β, μ_β is viscosity of phase β, $P_\beta = P + P_{cap,\beta}$ is the pressure in phase β (sum of a reference phase pressure and capillary pressure), and $\underset{\sim}{g}$ is gravitational acceleration. The last term in equation (5) contributes only for gas phase flow and represents a binary diffusive flux, with D_{va} the diffusion coefficient for vapor in air. In a more complete treatment other diffusive fluxes can be considered (Hadley, 1982; Ertekin et al., 1983), but the strength parameters for diffusive fluxes applicable to Nevada Test Site tuffs are not well known at present. In the calculations reported here binary diffusion was neglected ($D_{va} = 0$).

Heat flux contains conductive and convective components

$$\underset{\sim}{F}^{(3)} = - K\nabla T - k \sum_{\beta=\ell,g} h_\beta \frac{k_{r\beta}\rho_\beta}{\mu_\beta} (\nabla P_\beta - \rho_\beta \underset{\sim}{g}) - D_{va} h_v \nabla \rho_v \qquad (6)$$

Here K is heat conductivity of the rock-fluid mixture, h_β is specific enthalpy of phase β, and h_v and ρ_v are vapor specific enthalpy and density, respectively.

The transport equations given above need to be complemented with constitutive relationships, which express all parameters as functions of a set of primary thermodynamic variables. The thermophysical properties of water substance are accurately represented by the steam table equations, as given by the International Formulation Committee (1967). Because of the strong suction pressures encountered in desaturating tuff, vapor pressure lowering effects can be very large. These are represented by Kelvin's equation (Edlefsen and Anderson, 1943).

$$P_v(T, S_\ell) = P_{sat}(T) \cdot \exp\left(\frac{P_{cap}(S_\ell)}{\rho_\ell R(T + 273.15)}\right) \qquad (7)$$

Air is approximated as an ideal gas, and additivity of partial pressures is assumed for air and vapor, $P_g = P_v + P_a$. The viscosity of air-vapor mixtures is computed from a formulation given by Hirschfelder et al., (1954), but using steam table values for vapor viscosity instead of approximations from kinetic gas theory. Henry's law was assumed for solubility of air in liquid water. Capillary pressures and relative permeabilities will usually depend on phase saturations, but more general relationships (e.g. temperature dependence) are possible. At present no allowance is made for hysteresis.

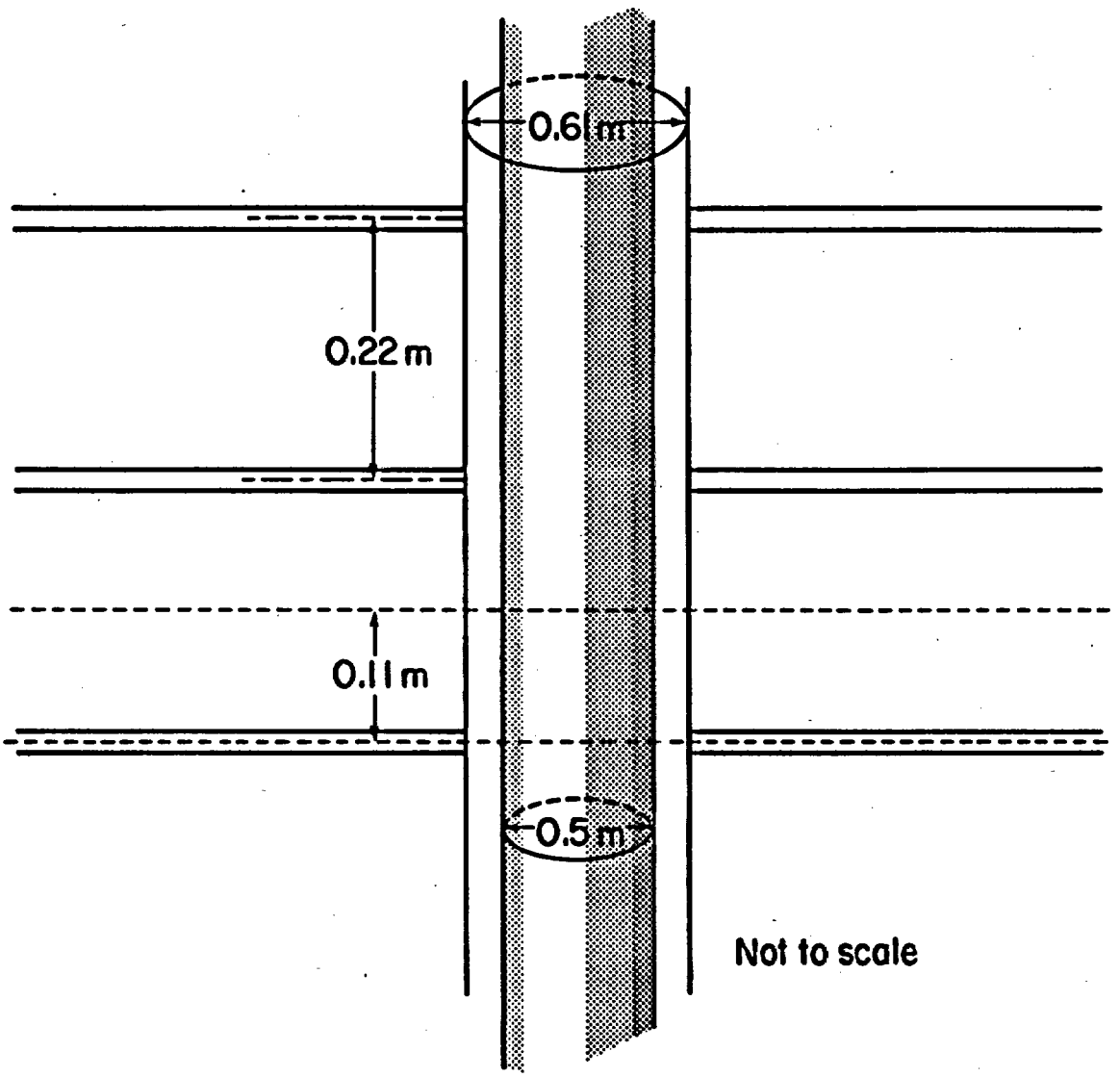

Figure 1. Idealized emplacement configuration. An infinite linear string of waste packages is intersected by fractures with 0.22 m spacing.

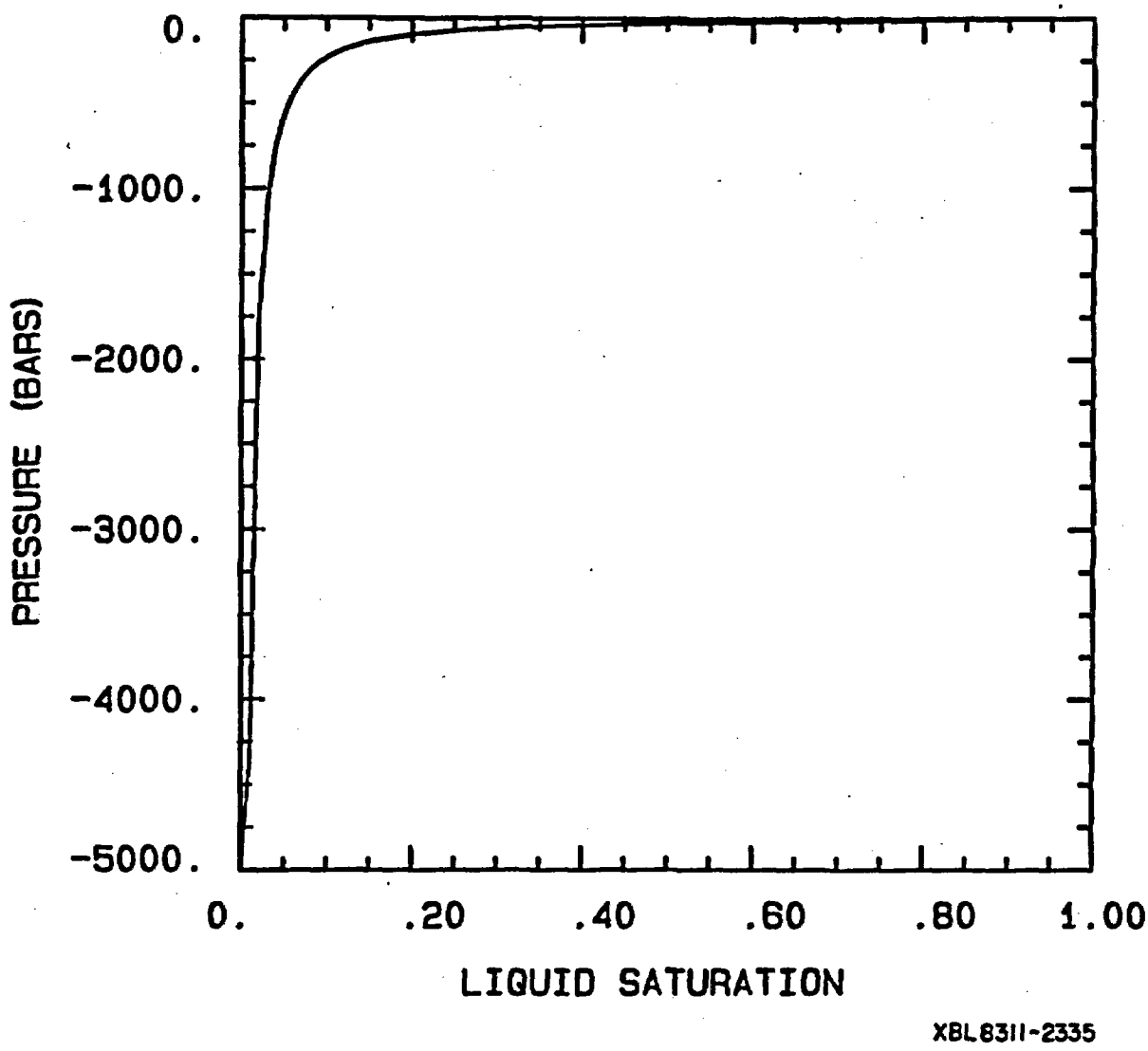

Figure 2. Suction pressure of tuff matrix.

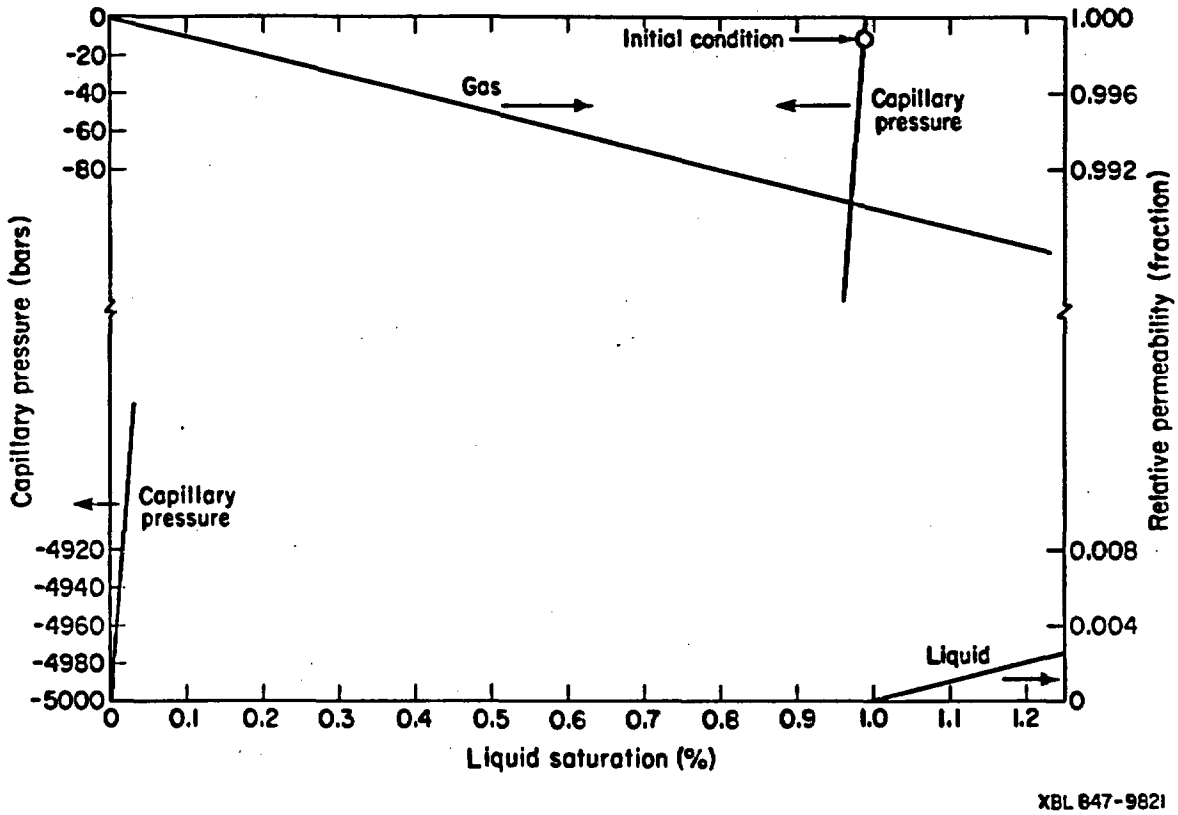

Figure 3. Hypothetical characteristic curves in the fractures (Case 1; liquid immobile in fractures).

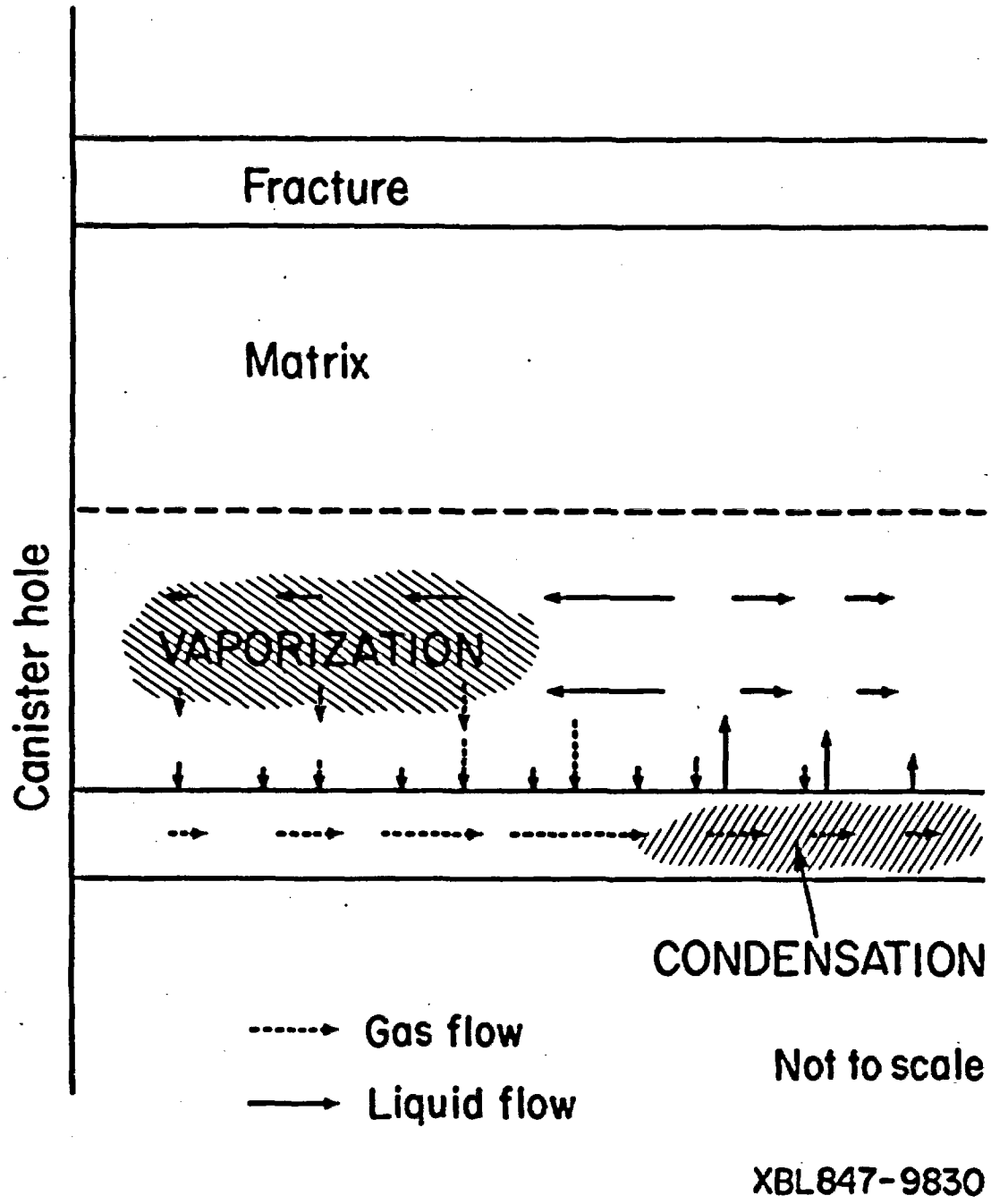

Figure 4. Response of fractured porous medium to heat load for case with immobile liquid in fractures.

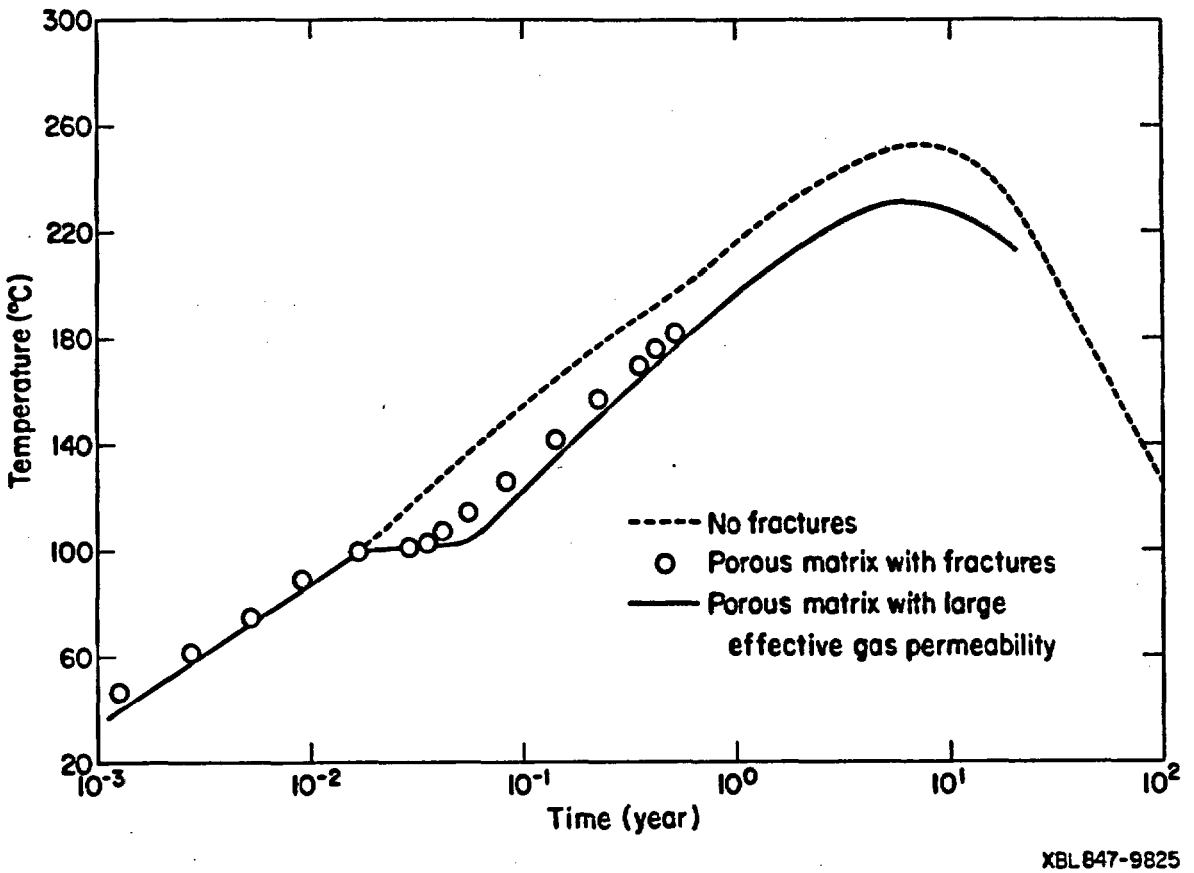

Figure 5. Simulated temperatures at a distance of r = 0.3355 m from the canister centerline (Case 1; liquid immobile in fractures).

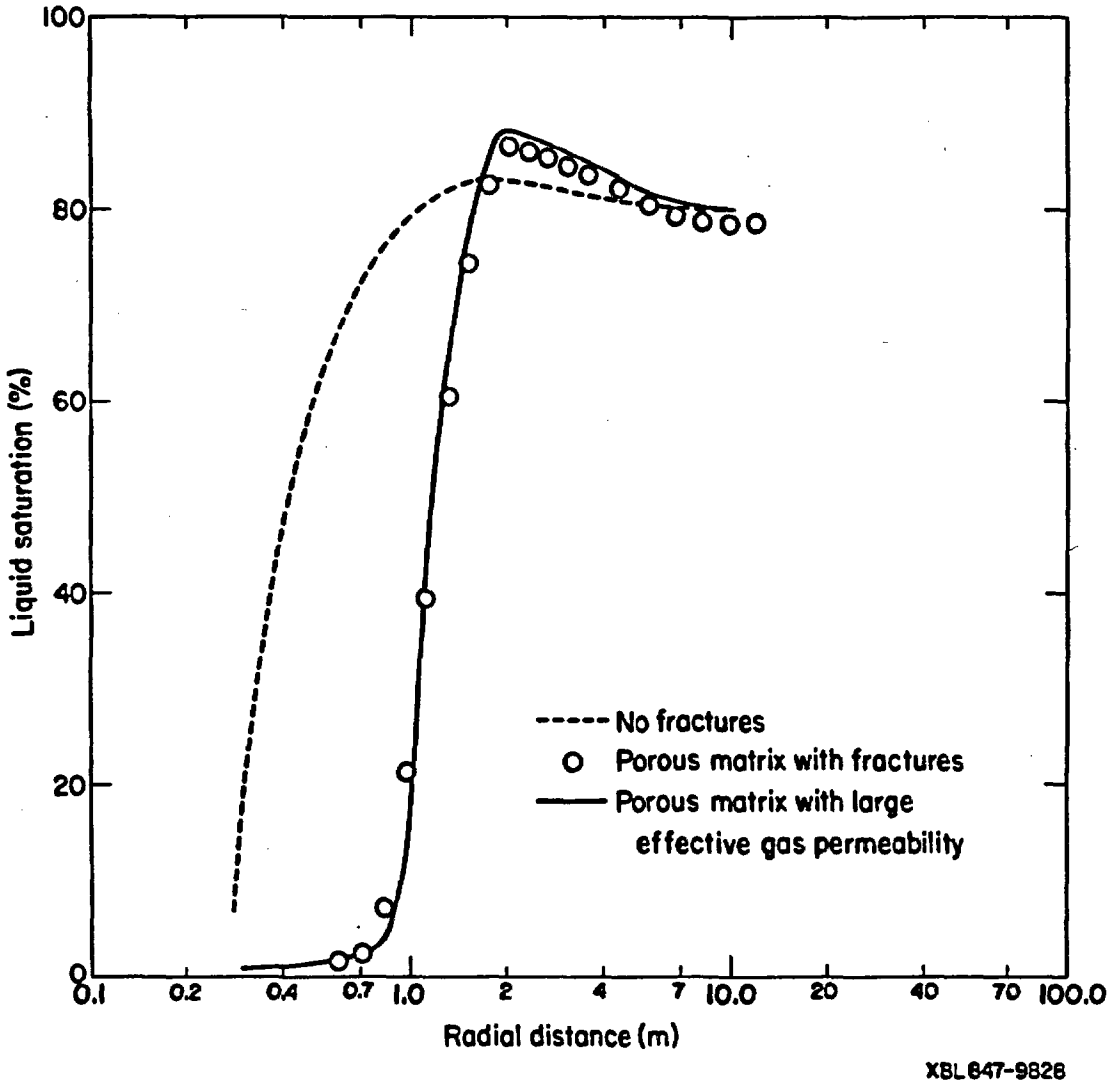

Figure 6. Simulated liquid saturation profiles at t = 160 days (Case 1; for the fractured medium an average of fracture and matrix saturations is plotted).

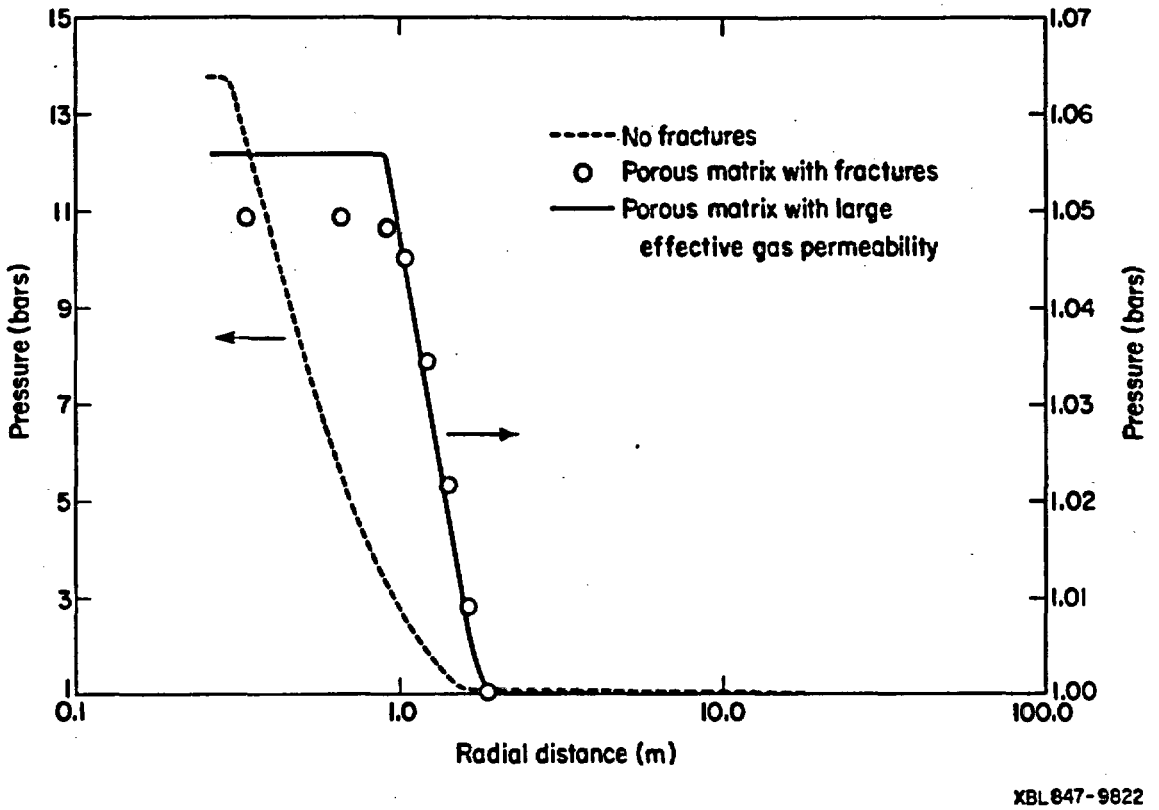

Figure 7. Simulated pressure profiles at t = 160 days (Case 1; for the fractured medium the pressure in the fractures is plotted; note the different scales!)

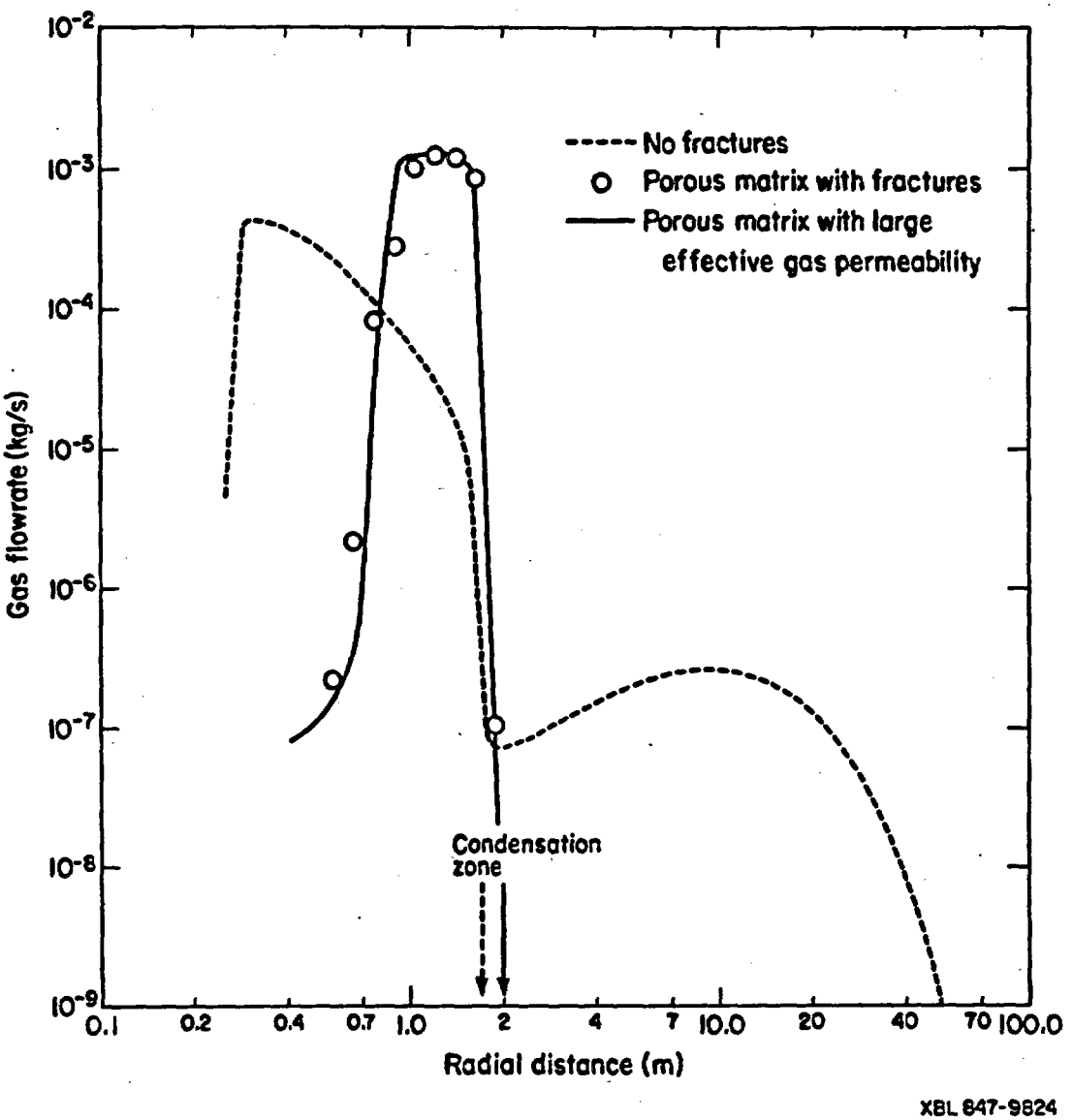

Figure 8. Simulated rates of radial gas flow per waste package at t = 160 days (Case 1).

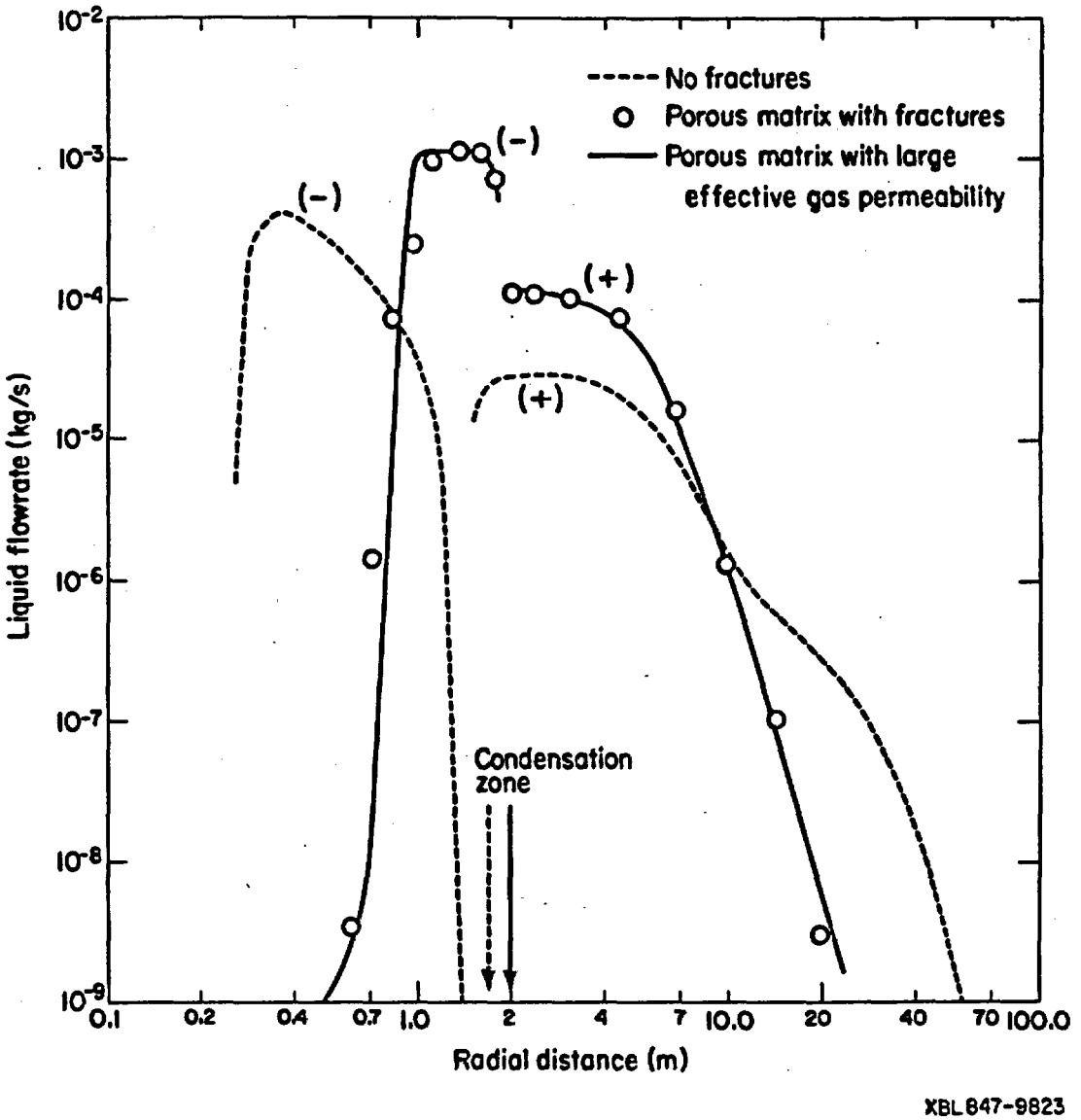

Figure 9. Simulated rates of radial liquid flow per waste package at t = 160 days (Case 1; a "-" sign indicates flow towards the waste packages).

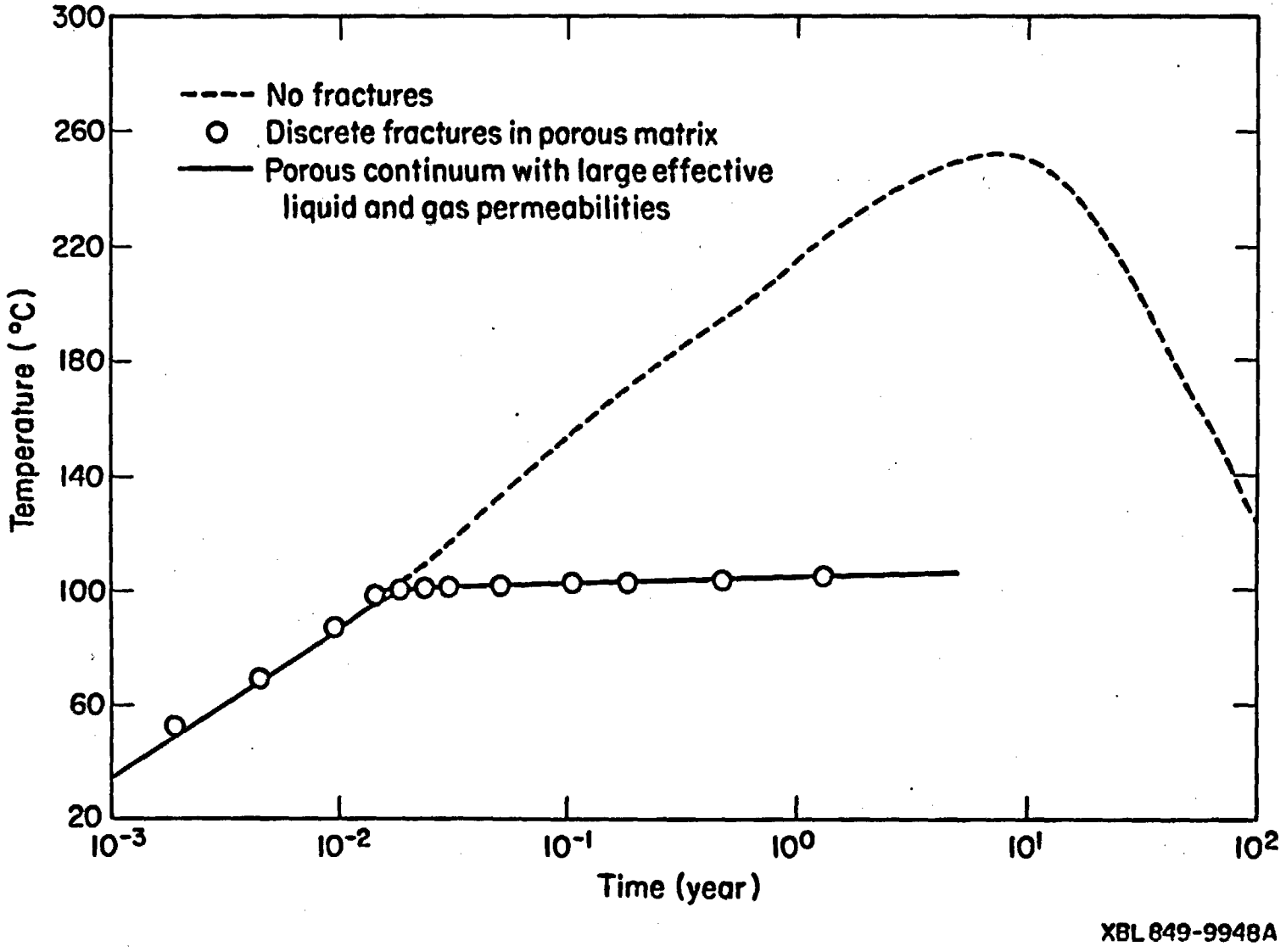

Figure 10. Simulated temperatures at a distance of r = 0.3355 m from the canister centerline (Case 2; liquid mobile in fractures).

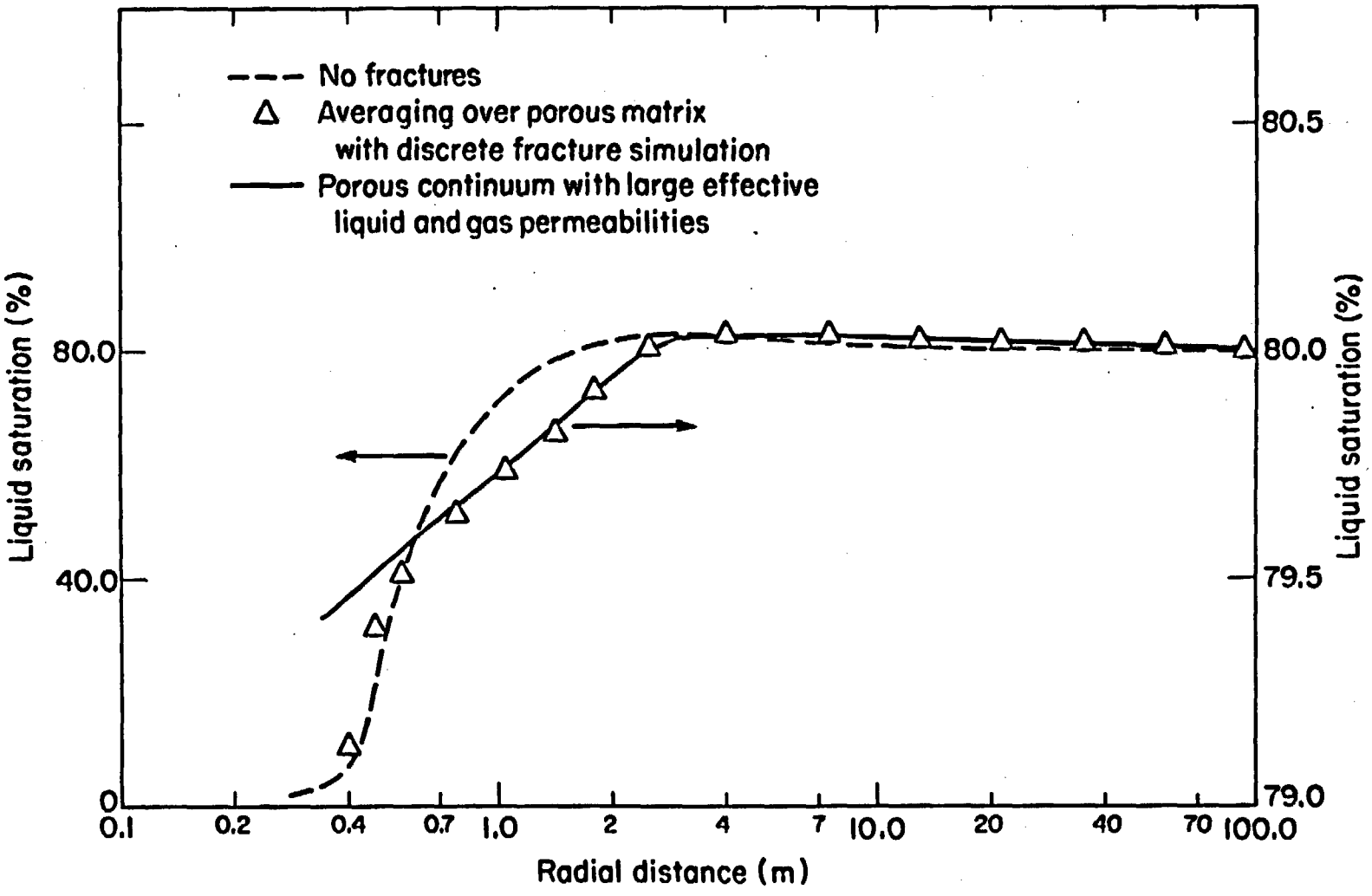

Figure 11. Simulated liquid saturation profiles at t = 1 year (Case 2; note the different scales!).

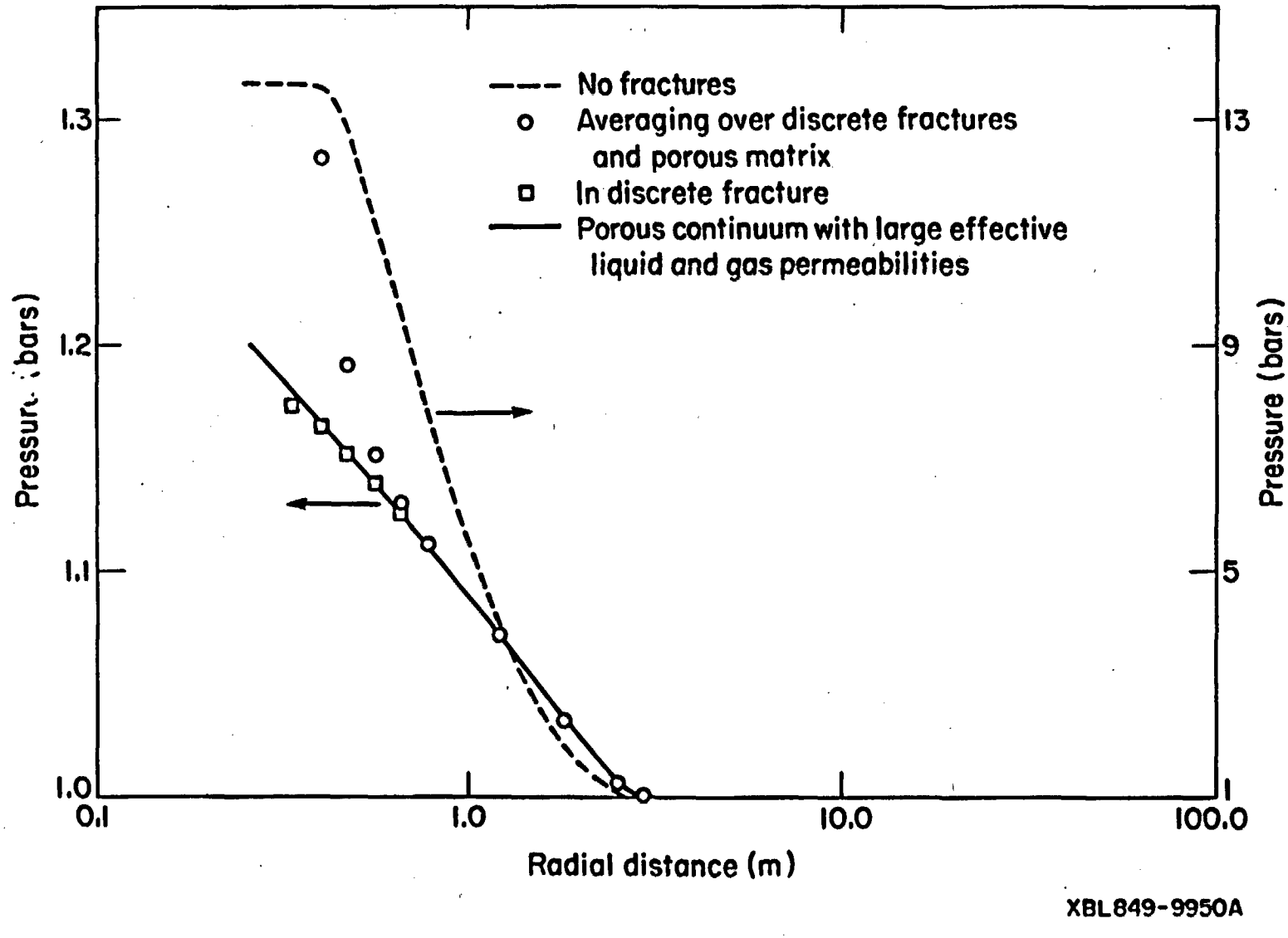

Figure 12. Simulated pressure profiles at t = 1 year (Case 2; note the different scales!).

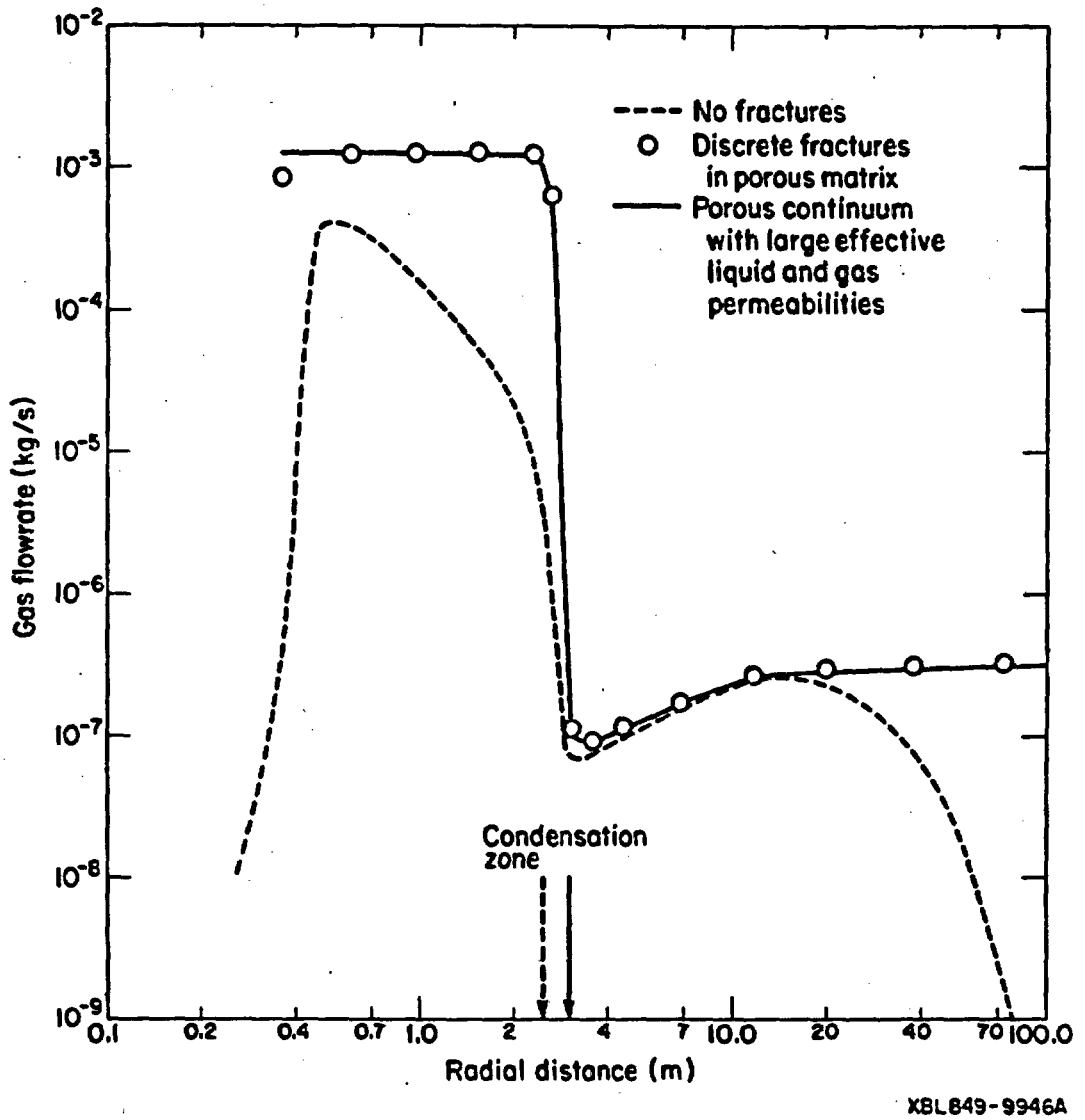

Figure 13. Simulated rates of radial gas flow per waste package at t = 1 year (Case 2).

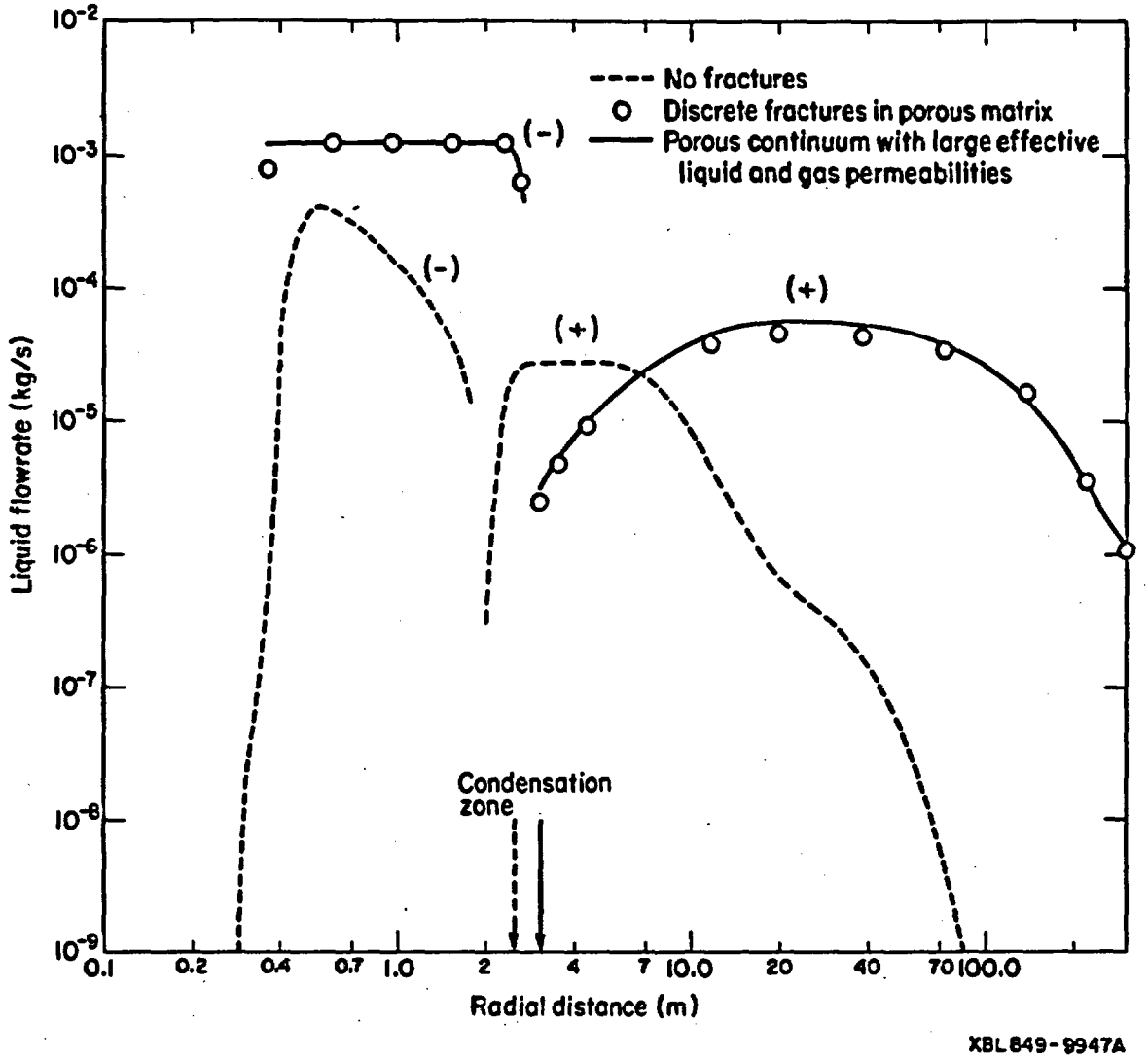

Figure 14. Simulated rates of radial liquid flow per waste package at t = 1 year (Case 2, a "-" sign indicates flow towards the waste packages).